Thermodynamic Investigation of Titanium Hydride Formation from Reduction of Titanium (Ⅳ) Chloride with Magnesium Hydride in Presence of Hydrogen Atmosphere

Mohammad Rezaei Ardani[1], Ahmad Fauzi Mohd Noor[1], Sheikh Abdul Rezan Sheikh Abdul Hamid[1*], Abdul Rahman Mohamed[2], Hooi Ling Lee[3], Ismail Ibrahim[2]

[1] School of Materials and Mineral Resources Engineering, Universiti Sains Malaysia, Nibong Tebal

[2] Mineral Research Centre, Mineral and Geoscience Department Malaysia, Ipoh, Perak

[3] Nanomaterials Research Group, School of Chemical Sciences, Universiti Sains Malaysia, Penang, Malaysia

[1*] Corresponding author: srsheikh@usm.my

Abstract

Thermodynamic assessment and experimental investigation for formation of titanium hydride (TiH_2) from reduction of titanium tetrachloride ($TiCl_4$) with magnesium hydride (MgH_2) were carried out under hydrogen atmosphere. In this method, TiH_2 production at low temperature was investigated, which can be used for further dehydrogenation process in titanium powder metallurgy. The effects of temperature, time, amount of titanium trifluoride (TiF_3) as catalyst, and ball milling time of MgH_2 on reduction process were evaluated. The range of each parameters were set to 250-350°C for temperature, 2-4 hr for reaction time, 4-10 wt% for TiF_3, and 1-2 hr for ball milling time. The phase transformations after reduction process were studied by X-ray diffraction (XRD) and energy-dispersive X-ray (EDX) analyziz. The morphology of powders was analyzed by scanning electron microscope (SEM). The results showed that titanium trichloride ($TiCl_3$) was formed as major product in experiments for the above conditions. However, with increasing the reaction time above 10hr, characterization study of the final products confirmed the formation of TiH_2 as major product. Our

findings indicated that producing of TiH_2 from reduction of $TiCl_4$ with MgH_2 at low temperature was feasible and could lead to low cost synthesis method for TiH_2 for titanium powder production.

Keyword: *Powder Metallurgy, Titanium, Titanium Hydride, Thermodynamic assessment*

Introduction

Titanium (Ti) and its alloys have been used in many industries such as aerospace, biomedical, power generation and structural applications due to properties such as low density, high temperature capabilities, high strength to density ratio, outstanding resistance to corrosion and high toughness in aggressive environment [1-4]. The demand to use Ti especially in aerospace industry is ever increasing nowadays; however, the high production costs of Ti is a major challenge [5], which makes the use of Ti restricted comparing to metals such as aluminum or steel [6].

The main problems in the industrial methods of Ti production with Kroll process and Hunter process [7], are the long processing time, high temperature and high energy consumption [8], which resulted in high cost of titanium in many industrial applications [9 ,10]. Several researchers [11-17] tried to develop new methods to produce titanium powder with powder metallurgy techniques in order to lower the production costs. Some of these processes such as hydrogen assisted magnesiothermic reduction (HAMR) and direct reduction of Ti-slag (DRTS) are using TiO_2 as a precursor [11-13]; however, the base material in TiRO^{TM} and Armstrong processes to produce Ti metal is $TiCl_4$ [14-17].

Whereas, reduction of chlorine content in $TiCl_4$ is more convenient comparing to remove oxygen from TiO_2, the Ti powder from $TiCl_4$ precursor is more pure considering the oxygen content. Besides, the chlorine by-products such as $TiCl_3$ can participate in the production process, while the oxide composition in processes using TiO_2 can make the process more complicated by formation of high melting point oxides [12, 16]. On the other hand, $TiCl_4$ is considerably corrosive and volatile gas. In addition, the nature of processes which use $TiCl_4$ is liquid to solid process and the morphology and particle size control are very challenging in this condition [16]. As a result the authors proposed an optimized method to improve the Kroll process via low temperature chlorination [18-19] and electrochemical reduction via TiS_2 [20] and use the obtained $TiCl_4$ as precursor to produce TiH_2 powder from the reduction process with metal hydrides at lower temperature with gas-solid reaction [21-23]. Hydrogen can then be easily removed from TiH_2 through a simple heat treatment in vacuum or inert atmosphere, thereby leaving pure Ti with extremely low levels of oxygen and hydrogen. TiH_2 is insoluble in water, resistant to dilute acid solutions, and has minimal or no solubility for other impurities [24].

Previous studies [25-27] investigated the magnesium–hydrogen reduction process of $TiCl_4$ to produce TiH_2 at 800 – 850 °C. The use of hydrogen gas in the process has several advantages such as decreases in reduction time, increases in the efficiency of magnesium usage and reduce further vacuum distillation stage time and temperature [28]. However, the elevated temperature of reduction step is still affecting the titanium production costs. The authors' proposed method [21-23] was carried out at lower temperature range in order to produce low cost titanium powder. In this study the $TiCl_4$ is reduced to TiH_2 with ball milled MgH_2 under hydrogen atmosphere at temperature range 250 – 350°C. The feasibility of this method is based on several fundamental principles which are discussed in details as follow.

Experimental

The $TiCl_4$ and MgH_2 is expected to react as Eq. 1 to produce TiH_2. The calculation for the amount of standard Gibbs free energy change (ΔG°) for Eq. 1 between 250-350°C shows negative value which indicates the reaction is thermodynamically feasible.

$$TiCl_4(g) + 2MgH_2 = TiH2 + 2MgCl_2 + H_2(g) \quad \Delta G^0 = -488.420 - 0.0393T\,(kJ/mol) \quad (1)$$

The schematic of experimental setup to perform the reaction between MgH_2 and $TiCl_4$ is illustrated in Fig. 1. Phosphorous pentoxide (P_2O_5) was used to absorb any moisture in the H_2 gas before entering the system. The flow rate of H_2 gas was monitored and controlled regularly during the experiment. Gaseous $TiCl_4$ and H_2 gas was passed through the quartz tube in the furnace. MgH_2 powder was ball milled under Ar gas with TiF_3 as catalyst to lower the dehydrogenation temperature of MgH_2 while increasing the surface area of the powder. Three different weight ratios between MgH_2 and TiF_3 were used including 4 -10 wt% of MgH_2 based on previous study [29]. The weight of MgH_2 with catalyst sample was constant at 1g. The milled powder was placed in a crucible at the center of the quartz tube at specified temperature. Residual exit gas from the tube was absorb with the hydrochloric acid (HCl) and neutralized by NaOH before excess gas was released to the atmosphere [22].

The experiments were carried out by varying four main factors with three distinct levels which are introduced as Table 1. Temperature was set to 250, 300 and 350°C, reaction time 120, 180 and 240 minutes, the amount of catalyst 4, 7 and 10 wt%, and the ball milling time 60, 90 and 120 minutes. All reduced samples were kept in inert atmosphere under Mylar film sandwich [30]. The phase compositions and morphology of the reaction products as well as the extent of reduction process were studied by X-ray Diffraction analysis using Cu-Kα radiation with the wavelength of λ=1.5404 Å (XRD; Bruker D8-advance, USA). The surface morphology and the elemental

composition of the reaction product were studied by Scanning Electron Microscopy equipped with Electron Dispersive X-ray Spectroscopy (SEM/EDX; Tescan MIRA3, Czech Republic and ZEISS SUPRA 35VP, Germany).

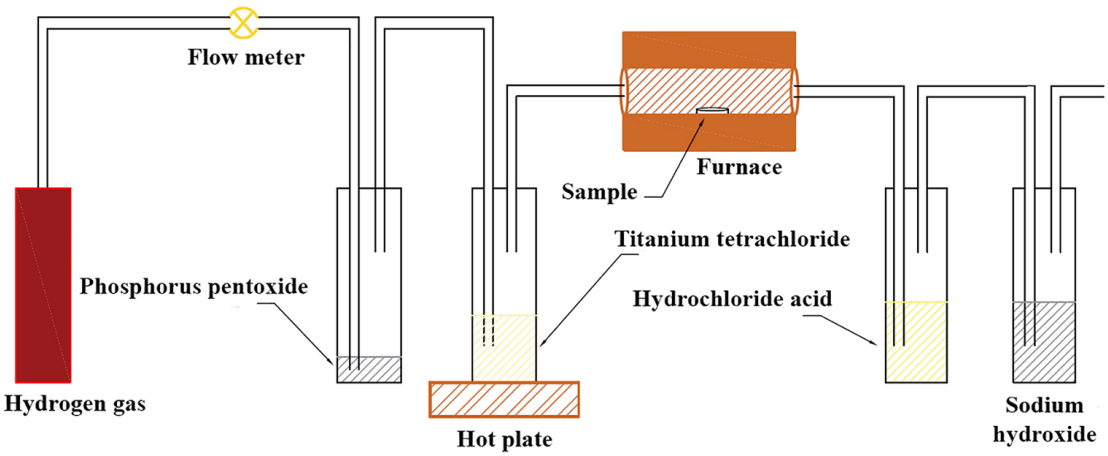

Fig. 1. Experimental Set-up. From the left to right: H_2 gas passed through the P_2O_5 till $TiCl_4$ scrubber.

Table 1. Experimental matrix: Factors and levels

Run	Factor 1	Factor 2	Factor 3	Factor 4		
	A:Temperature	B:Time	C:Catalyst Amount	D:Ball Milling Time	**$TiCl_3$ amount**	**Final powder weight**
	°C	Min	%wt	Min	(g)	(g)
1	250	120	4	60	0.27	1.76

2	250	120	10	60	0.13	1.67
3	350	240	10	60	0.29	2.36
4	250	120	4	120	0.13	1.75
5	250	240	10	120	0.20	1.71
6	350	240	4	60	0.44	2.52
7	300	180	7	90	0.47	2.43
8	250	240	4	120	0.10	1.76
9	350	120	4	120	0.16	2.66
10	350	120	10	120	0.18	2.35
11	350	120	10	60	0.43	2.55
12	250	240	10	60	0.15	1.76
13	250	120	10	120	0.13	1.72
14	300	180	7	90	0.66	2.59
15	350	240	10	120	0.53	2.67

16	300	180	7	90	0.60	2.43
17	350	120	4	60	0.10	1.59
18	350	240	4	120	0.67	2.82
19	250	240	4	60	0.17	2.00

Results and Discussion

Thermodynamic calculations

In order to evaluate the effect of temperature, partial pressure of H_2 and Cl_2 gas was calculated over Ti-Cl-H predominance diagram in Fig. 2 at a fixed partial pressure of $P_{Cl_2} = 1\times10^{-30}$ atm and $P_{Cl_2} = 1\times10^{-35}$ atm. Fig. 2(a) shows that Ti, Cl and H were stable phases as$TiCl_3$, $TiCl_2$ and TiH_2 when the H_2 pressure of 1 atm and the temperature ranged between 250-350°C. Fig. 2(b) indicates that with the decrease in P_{Cl_2} the TiH_2 stability area will extend to lower temperatures and it was stable phase. This particular distinction between the two diagrams represents an important factor over the experimental conditions necessary to obtain TiH_2, which is P_{Cl_2} should be low enough. $TiCl_3$ can be produced from the reaction between $TiCl_4$ and MgH_2 as Eq. 2.

$$2TiCl_4(g) + MgH_2 = 2TiCl3 + MgCl_2 + H_2(g) \quad \Delta G^0 = -415.140 + 0.197T\,(kJ/mol) \quad (2)$$

Although Eq. 1 is thermodynamically feasible, to maintain TiH_2 formation, $TiCl_3$ is only stable at temperature above 350 °C for P_{H_2} of 1 atm and P_{Cl_2} below 1×10^{-30} atm. In contrast, Fig. 2(b) demonstrates that at lower P_{Cl_2}, TiH_2 was stable phase above 250°C. Moreover, with increasing P_{H_2} to 10 atm, TiH_2 was predominant even at lower temperatures. With the presence of H_2 around 1 atm was critical to have TiH_2 at lower temperatures. This is the main reason why there was a need to carry out the reduction process in the presence of H_2 atmosphere instead of inert atmosphere like previous studies [22, 23] to facilitate the reduction process.

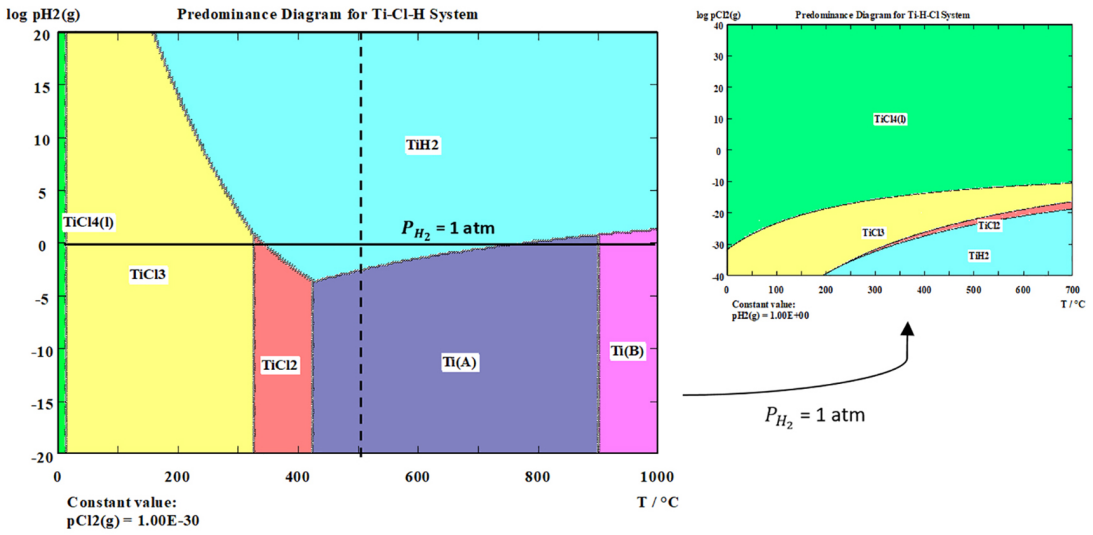

(a)

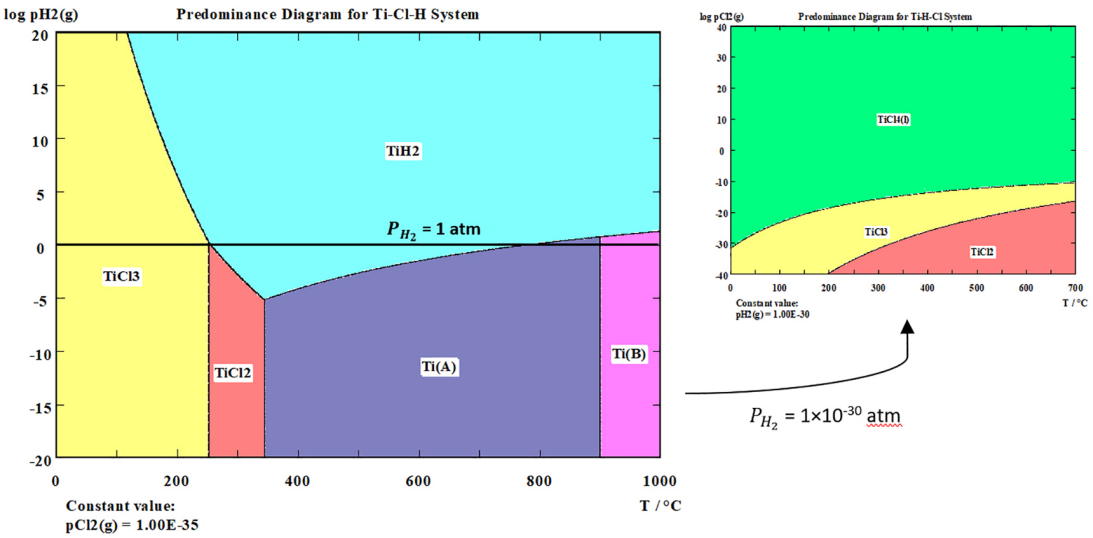

(b)

Fig. 2. Predominance Diagram for Ti-Cl-H system at a constant partial pressure of Cl_2 (a) P_{Cl_2}= 1×10^{-30} atm and (b) P_{Cl_2}= 1×10^{-35} atm

Gibbs minimization diagrams were developed to study the possible phase formation with the change in molar ratio of $TiCl_4$:MgH_2. Based on experimental conditions, the MgH_2 amount was set at 90% of the input materials with 10% of TiF_3 as catalyst in the calculations. Also, the constant amount of H_2 equivalent to 2 kmol was considered in the calculations. The main reason for these calculations was to consider the varying amount of $TiCl_4$ over time during the reduction process. Therefore, different reaction times caused different components to be reacted. The HSC Chemistry software v6.0 (Outokumpu Research Oy, Finland) with Gibbs energy minimization method was applied to analyze the possible equilibrium phase compositions during the reactions [31]. The main reaction to synthesize TiH_2 from $TiCl_4$ was given in Eq. 1. On the other hand, Eq. 3 and 4 indicate that $TiCl_3$ was a more favourable route than $TiCl_4$ to react with MgH_2 due to its lower ΔG° compared with Eq. 1. However, one of the important challenges in this process was the proper molar ratio of reactants. In the presence of excess $TiCl_4$, there was a possibility that the produced TiH_2 may react with $TiCl_4$ to form $TiCl_3$ as Eq. 5.

$$2TiCl_4(g) + 2H_2(g) = 2TiCl3 + 2HCl(g) \quad \Delta G^0 = -96.820 + 0.170T\,(kJ/mo) \quad (3)$$

$$2TiCl_3 + 3MgH_2 = 2TiH2 + 3MgCl_2 + H_2(g) \quad \Delta G^0 = -575.980 - 0.0679T\,(kJ/mo) \quad (4)$$

$$5TiCl_4(g) + TiH_2 = 6TiCl3 + 2HCl(g) \quad \Delta G^0 = -524.460 + 0.510T\,(kJ/mo) \quad (5)$$

The stoichiometric molar ratio for the $TiCl_4$ to MgH_2 was 1:2 according to Eq. 1. Fig. 3 indicates the equilibrium phase composition for the stoichiometric condition. Totally, the major products were TiH_2, $MgCl_2$ and H_2 according to Eq. 1. It is to be noted, the presence of MgF_2 in the final composition, is related to the reaction between TiF_3 and MgH_2 to produce MgF_2 and TiH_2 [32], which was almost negligible.

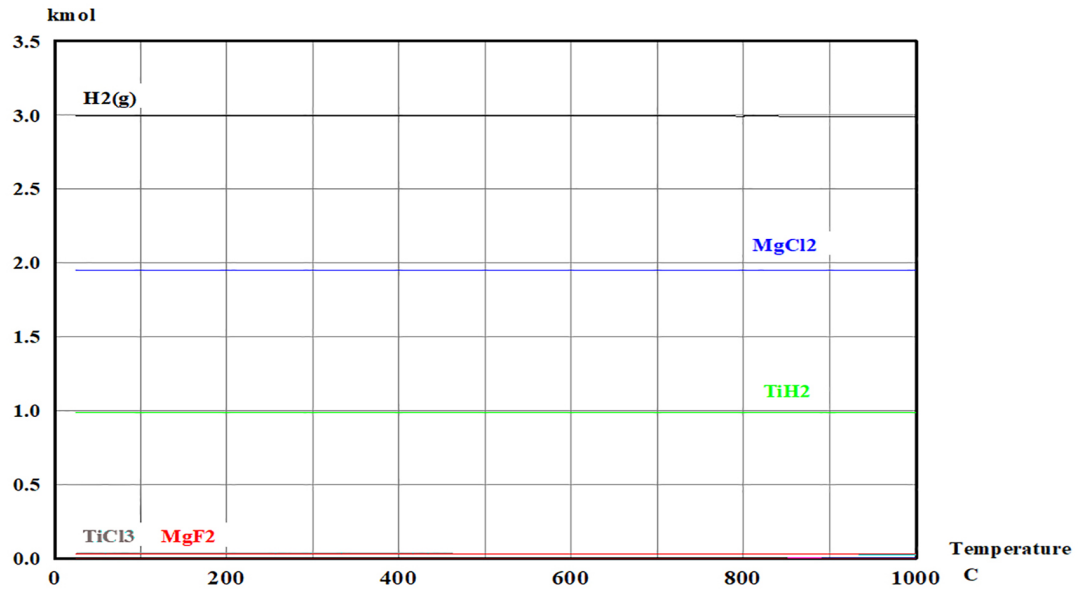

Fig. 3: Theoretical equilibrium phase composition calculated for the stoichiometric ration of $TiCl_4$: MgH_2 : = 1:2 and H_2 at 1 kmole.

The predicted phases with the increase in molar ratios of $TiCl_4$ to MgH_2 to 3:1 were represented in Fig. 4. As calculated, with an increase in molar ratio of reactants, the $TiCl_3$ phase formed rather than TiH_2. As expected, TiH_2 and $MgCl_2$ were formed at lower temperatures. However, the ΔG° for the reaction of Eq. 6 was more negative than Eq. 3 above 200°C and the reaction will proceed to produce H_2 and $TiCl_4$. In addition, the produced TiH_2 can react via Eq. 5 and there was no TiH_2 formed calculated in the equilibrium composition diagram. In essence, the main reaction between $TiCl_4$ and MgH_2 via Eq. 2 was occurring only. Nevertheless, the formation of TiH_2 was possible through reaction between MgH_2 and $TiCl_4$; however, the molar ratio of reactants was critically important to ensureTiH_2 formed.

$$2TiCl_3 + 2HCl(g) = 2TiCl4(g) + H_2(g) \quad \Delta G^0 = 47.97 - 0.159T\,(kJ/mo) \quad (5)$$

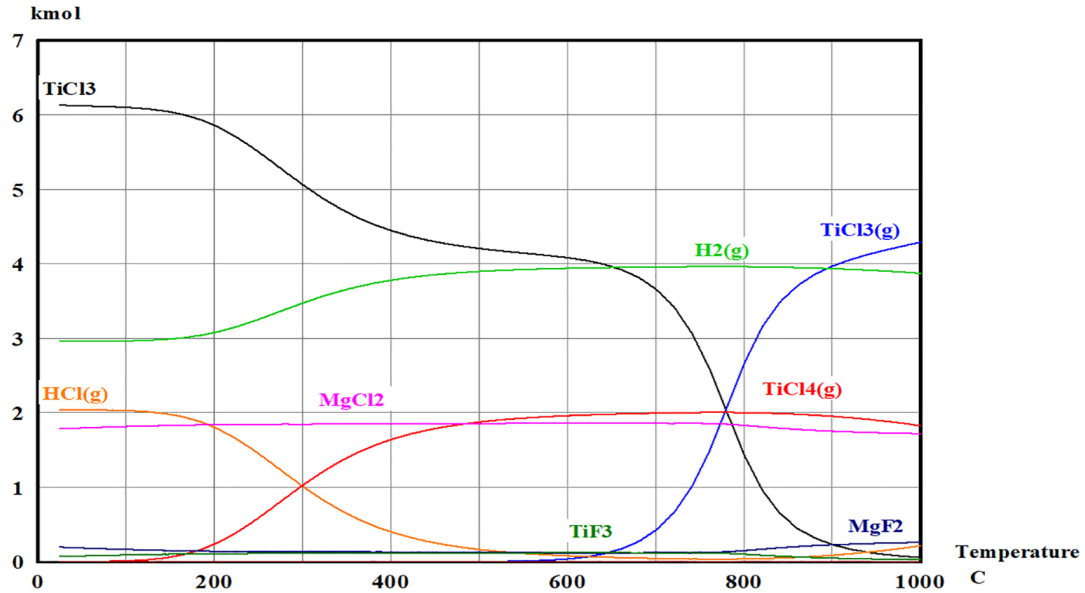

Fig. 4: Theoretical equilibrium phase composition calculated for $TiCl_4$: MgH_2 : H_2 = 6:2:2

In regard to the decreasing of temperature range to formed TiH_2, the thermodynamics results indicate with increase in P_{H_2} or decrease in P_{Cl_2} in the system, TiH_2 was the predominant phase. Based on the thermodynamic evaluation, it was clear that reduction of $TiCl_4$ with MgH_2 in H_2 atmosphere was feasible to form selectively TiH_2 within a particular temperature range, as demonstrated through the Gibbs minimization calculations.

Phase transformation

Regarding the phase transformations during MgH_2 reduction of $TiCl_4$, the thermodynamic calculation shows that the formation of equilibrium phases is highly dependent on the molar ratio of reactants. In this study, the final products after reduction process were analyzed by XRD to determine the phases. Despite the results from thermodynamic assessment, which shows that final equilibrium phases should be $MgCl_2$, TiH_2 and $TiCl_3$, the XRD results showed that the actual reaction products were mainly $MgCl_2$ and $TiCl_3$. In this case, the final products significantly affected by the factors including molar ratio of $TiCl_4$:MgH_2, temperature, time, and the P_{H_2} which can influence the reactions kinetics [33]. Furthermore, the $TiCl_4$ gas was carried into the furnace with H_2 and there was no actual data about the real ratio of $TiCl_4$:H_2 gas in the furnace during the reaction in the literature. According to Fig. 5. XRD

results show that the main phases was $TiCl_3$ and $MgCl_2$ or $MgCl_2.(H_2O)_X$. Although the samples were kept in Mylar film, however for the XRD analysis the samples were removed from Mylar which then can be absorbed moisture as $MgCl_2$ is very hygroscopic according to Eq. 7 and 8 [34, 35].

$$MgCl_2.4H_2O + 2H_2O(g) = MgCl_2.6H_2O \quad \Delta G_0^f = -2113.50\,(kJ/mol)\ at\ T = 298.15K \quad (7)$$

$$MgCl_2.2H_2O + 2H_2O(g) = MgCl_2.4H_2O \quad \Delta G_0^f = -1623.77\,(kJ/mol)\ at\ T = 298.15K \quad (8)$$

In addition, the presence of MgH_2 in the XRD results at T=250^{o}C, shows that the reaction time was inadequate. The amount of $TiCl_3$ phase in the final powder were calculated based on the Rietveld analysis. According to table 1, it can be concluded with the increase in the temperature from 250 to 350°C more $TiCl_3$ were formed. Also, the final powder weight showed that with the increase in temperature and reaction time, more $TiCl_4$ were reacted.

As it was mentioned, previous studies [29, 32] reported that the mechanical milling of MgH_2 with TiF_3 as the catalyst can reduced the dehydrogenation temperature. The higher the amount of catalyst amount and ball milling time resulted in the decrease in dehydrogenation temperature of MgH_2. The comparison between the XRD data indicated that with the increase in temperature from 250°C to 350°C, the intensity of MgH_2 peaks were weaker which represented the increase in MgH_2 reaction with $TiCl_4$. Also, the presence of Mg peaks at 350°C confirmed the dehydrogenation of MgH_2 at this temperature. The Mg content at 350°C was also included in the amount of unreacted MgH_2 on the XRD patterns in Fig. 5. It should be pointed that dehydrogenation of MgH_2 during the reduction process increases the P_{H_2} in the system, which have the positive effect on the formation of TiH_2 according to Fig. 2. The unstable TiH phase was only observed as low intensity peaks in the experiments at 350°C and 4hrs, such as run #18 according to Fig. 5. The low TiH was attributed to the reactants molar ratio and the formation kinetics of TiH_2 [33]. Moreover, the predominance diagrams of Ti-Cl-H indicates that the change in the P_{Cl_2} can be resulted in different stability area for $TiCl_3$ and TiH_2 at the temperature range of 250 - 350°C.

The XRD analyziz showed that with the increase in the reaction time and temperature the titanium hydride formation is observed. Given this, three different experiments were carried out for the 8, 10 and 12hrs. These experiments had two distinct differences. Based on the thermodynamic assessment from Fig. 2(a), temperature was set to 400°C to ensure the stability of TiH_2. In addition, the constant stoichiometry amount of $TiCl_4$ was added to the MgH_2 in crucible in the furnace to avoid the increasing in the ratio of the $TiCl_4$:MgH_2. The MgH_2 was milled for 60 min with 10%wt of TiF_3. The XRD results is shown in Fig. 6. As it can be seen, with the increase in reaction time to 8hrs the TiH

and TiH_2 phases were starting to form. Above 10 hrs the intensity of the TiH_2 and TiH phases is increased. Another interesting point of the XRD results is that there was no sign of $TiCl_3$ which shows in this conditions the $TiCl_3$ was also reacted to produce titanium hydride.

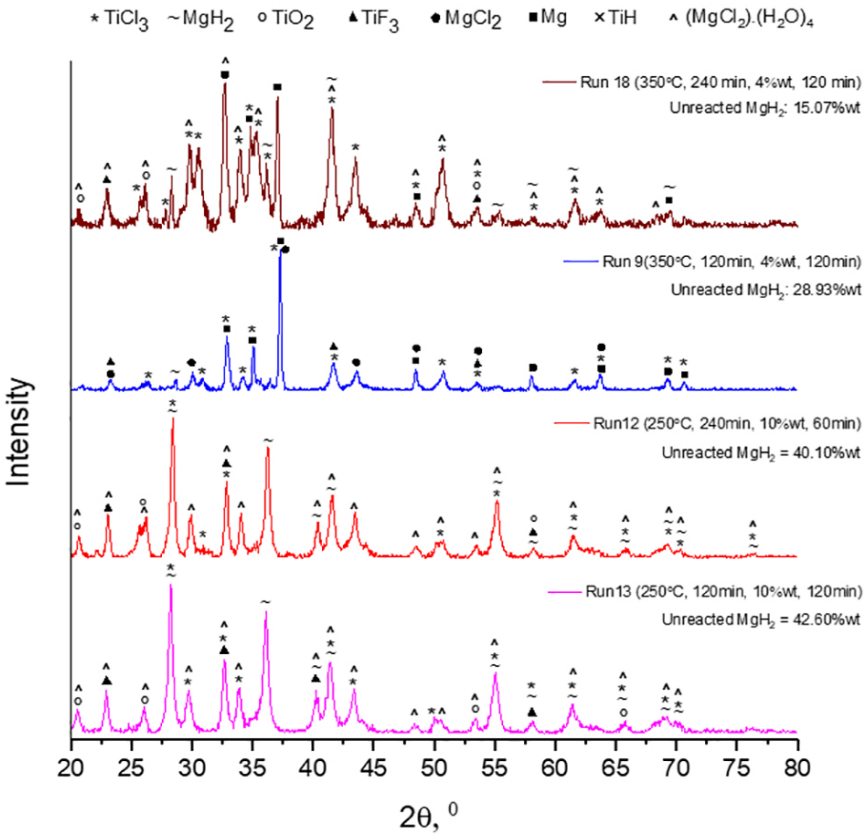

Fig. 5. XRD analysis data for the runs #9, #12, #13 and #18

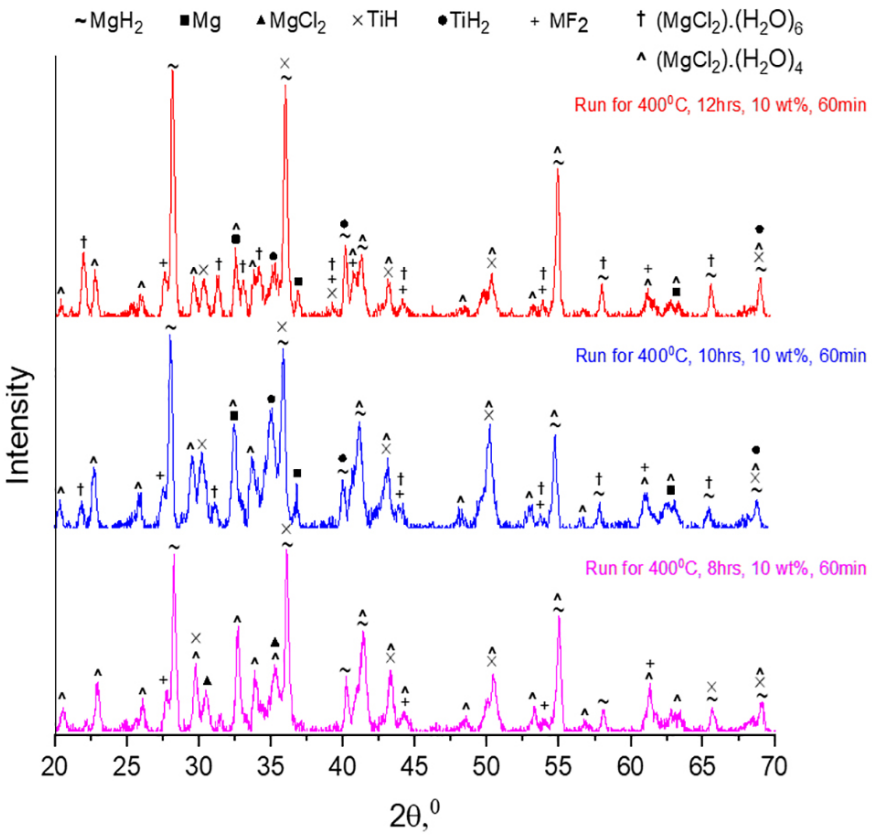

Fig. 6. XRD analysis data for the experiments at 8, 10 and 12hrs

Microstructural Characterization

The morphology and SEM/EDX analysis for the final powder after reaction between $TiCl_4$ and ball milled MgH_2 with the conditions listed in table 1, were investigated with provided in Fig. 7 and 9. According to the XRD analysis and the final weight of the powder, the morphology changed with an increase in temperature and reaction time as represented in Fig. 7. Fig. 7(a) shows that the morphology of the final product was agglomerated spherical particles for the experiments with lower temperature and reaction time, such as runs #4 and #5. With an increase in the temperature and reaction time, new phase with the angular shaped morphology is appeared such as runs #6, #7 and #18. At low temperatures and reaction times, the main phase is MgH_2 which can be seen as spherical shaped

powders which were partially sintered. With an increase in temperature the major change in the morphology is related to formation of new phase which is related to $TiCl_3$ and TiH_2 as shown from Fig. 7(c) to 6(e). It can be seen from Fig. 7(c) to 7(e) that spherical shape particles were almost disappeared and severely agglomerated powders were formed. In addition, due the formation of $(MgCl_2)(H_2O)_x$ phases, the needle shape morphology were detected in the final powders as it is indicated in Fig 7(e).

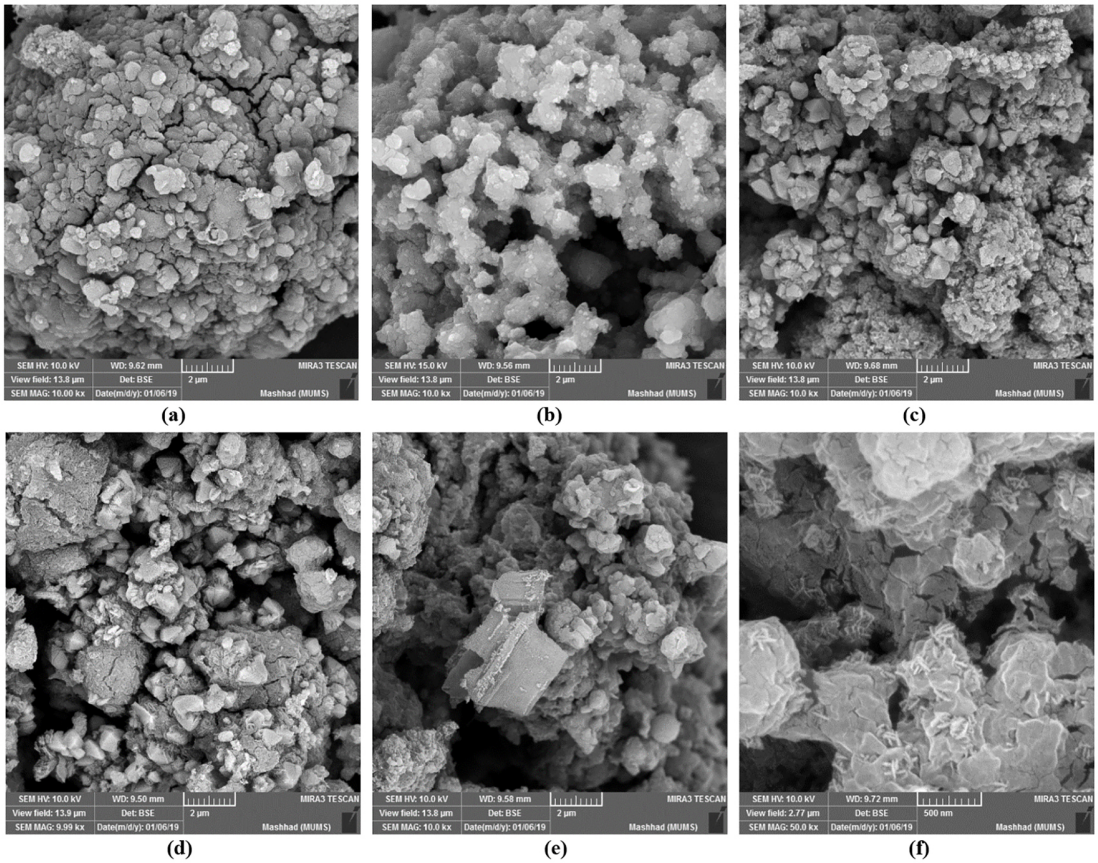

Fig. 7. SEM image of final powder (a) Run #4, (b) Run #5, (c) Run #6, (d) Run #7, (e) Run #18, (f) Run #13

Fig. 8 shows the SEM/EDX analysis which were confirmed by XRD analysis for the extent of reaction and product phases formed. For the samples reduced at 250°C, the EDX analysis showed different phases with low Ti and high Mg content. On the other hand, with an increase in temperature to 350°C, the phases with high Ti content were observed. Therefore, with the change in reaction condition more

Ti was reacted with MgH_2. In comparison between samples from run #9 and run #18, it was obvious that with the increase in reaction time, the higher Ti content phases were formed during the reaction.

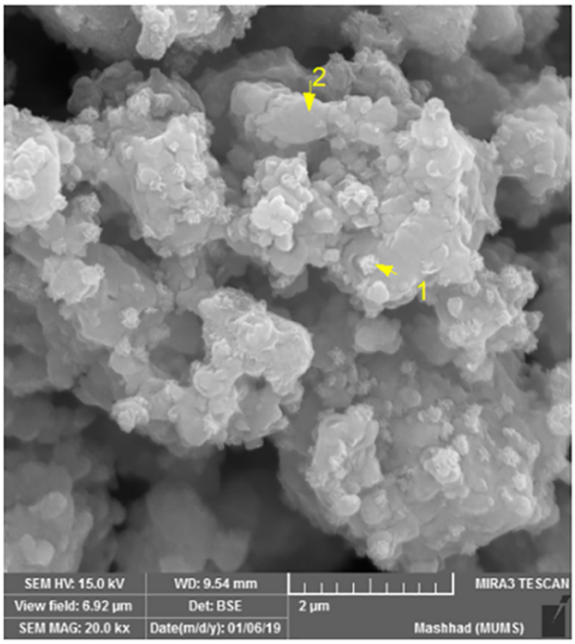

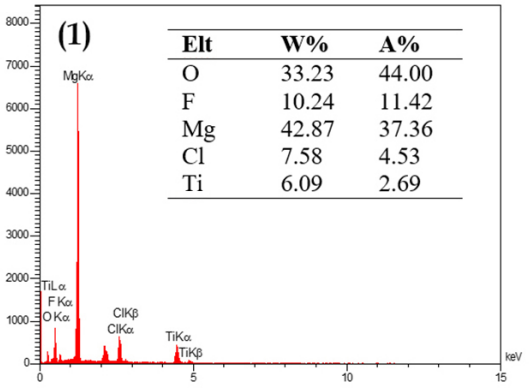

Elt	W%	A%
O	33.23	44.00
F	10.24	11.42
Mg	42.87	37.36
Cl	7.58	4.53
Ti	6.09	2.69

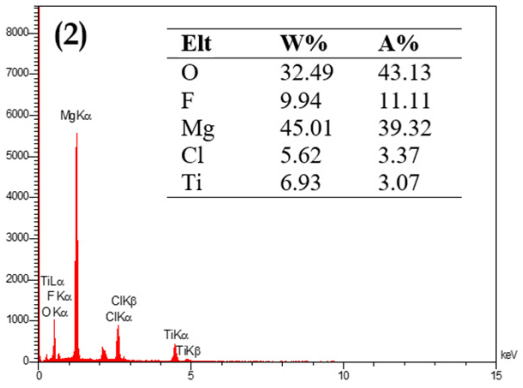

Elt	W%	A%
O	32.49	43.13
F	9.94	11.11
Mg	45.01	39.32
Cl	5.62	3.37
Ti	6.93	3.07

(a)

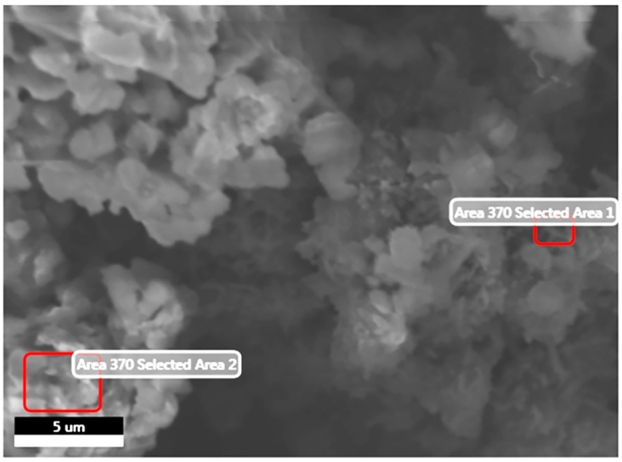
Area 370 Selected Area 1
Area 370 Selected Area 2
5 um

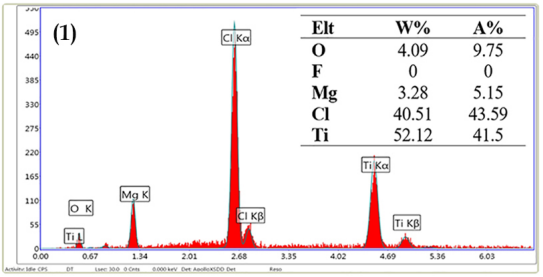
(1)
Cl Kα
Mg K
O K
Ti L
Cl Kβ
Ti Kα
Ti Kβ
Elt W% A%
O 4.09 9.75
F 0 0
Mg 3.28 5.15
Cl 40.51 43.59
Ti 52.12 41.5

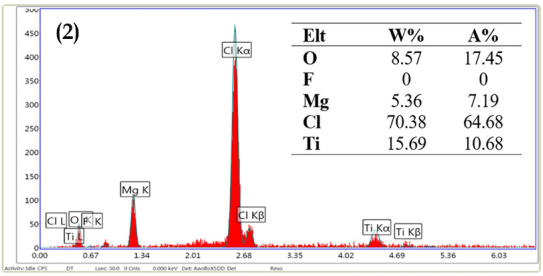
(2)
Cl Kα
Mg K
Cl L
O K
F K
Ti L
Cl Kβ
Ti Kα
Ti Kβ
Elt W% A%
O 8.57 17.45
F 0 0
Mg 5.36 7.19
Cl 70.38 64.68
Ti 15.69 10.68

(b)

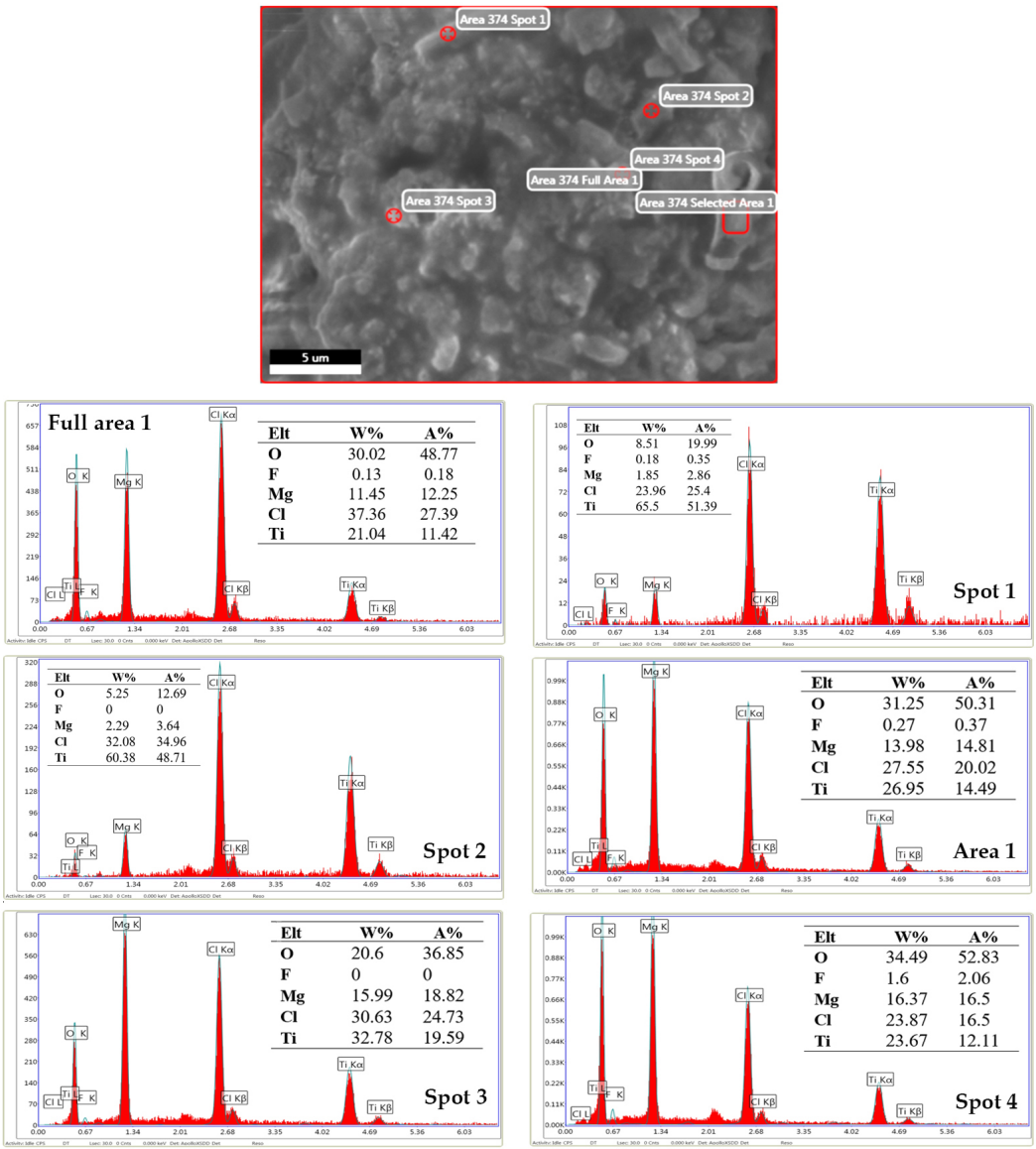

(c)

Fig. 8. EDX analysis of final powder (a) Run #5, (b) Run #9, (c) Run #18

As it was mentioned in the previous section, the XRD results showed that with an increase in reaction time the titanium hydride was formed. Fig. 9 represents the SEM/EDX analyziz for the sample reduced for 10hrs. In comparison with the morphology of the powders in Fig. 7, it is clear that new

large phase was formed in reaction for 10hrs and 400°C. Although the EDX analyziz showed Mg,Cl and O elements in the background, these elements related to the aggolomerated spherical phases in the matrix and the new phase is completely formed from Ti which is related to the formation of titanium hydride.

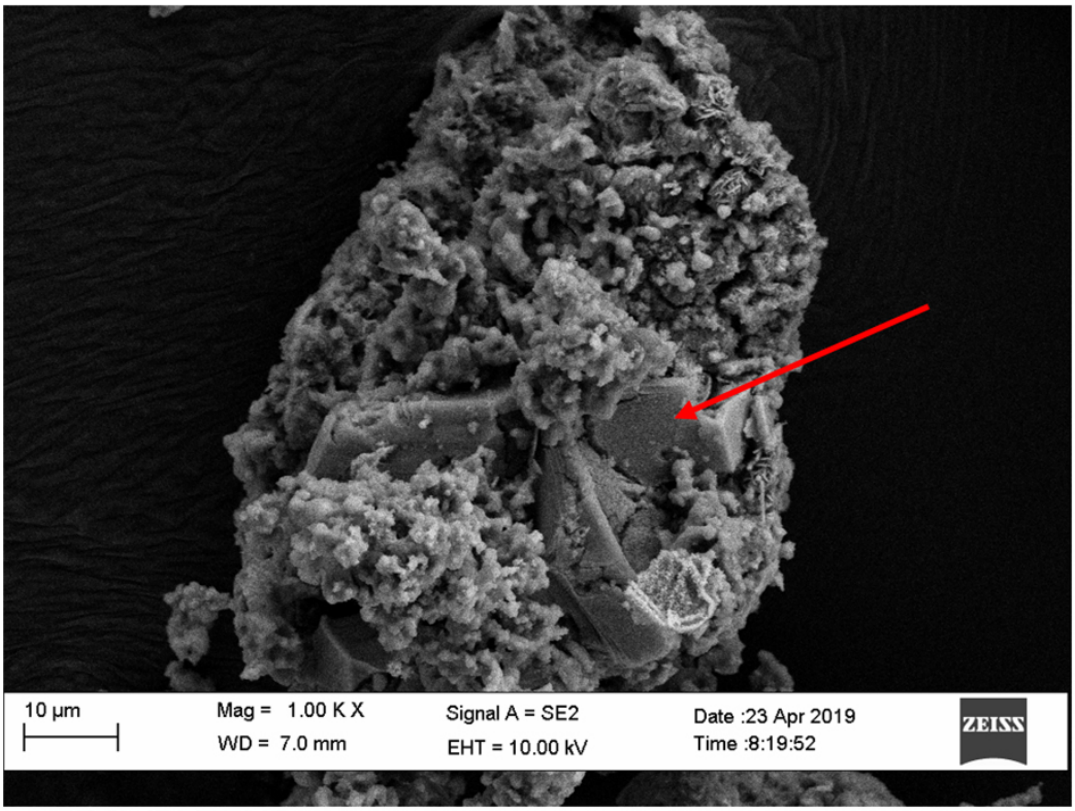

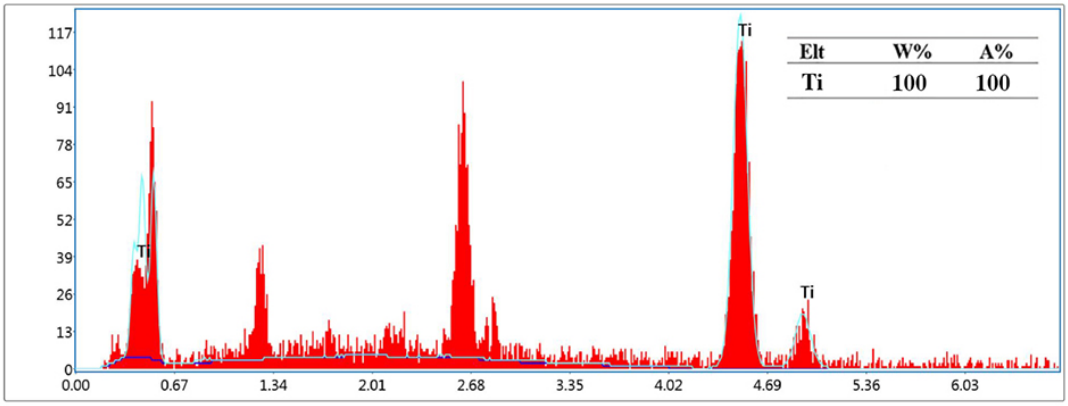

Fig. 9. EDX analysis of final powder for the experiment after 10hrs

The characterization of the final powders confirmed the formation of TiH_2 at low temperature through the reaction between $TiCl_4$ and ball milled MgH_2. Although, in the reactions at lower reaction times (below 4hrs), the main product phase was $TiCl_3$, in the experiments for longer reaction time above 10hrs the main phases were TiH and TiH_2. With respect to the chemical compositions of the products, the possible pathway to produce TiH_2 with this route was the formation of $TiCl_3$ at the beginning stages of the reduction process and then with an increase in reaction time above 10hrs and slight increase in temperature up to 400°C the reaction between $TiCl_3$ and remaining MgH_2 would result in formation of TiH_2.

Conclusion

Experiments have been conducted to synthesize TiH_2 from the reaction between ball milled MgH_2 and $TiCl_4$ gas in the presence of H_2 atmosphere. The investigated parameters were temperature, reaction time, amount of TiF_3 and ball milling time. The XRD analyziz of the products showed that the main phase of the reaction at the specified experimental condition in early stages of the reduction process was $TiCl_3$ rather than TiH_2. However, with an increase in reaction time above 10hrs, TiH and TiH_2 phases were formed. In addition, it was reported that with increase in the temperature and reaction time, more $TiCl_3$ was formed according to the conditions of run #10 and #11. On the other hand, with the increase in reaction time from 2hrs to 4hrs, TiH_2 phases was observable by XRD in run #18. The SEM/EDX characterization of the products indicated that at 250^{o}C, the main morphology observed was spherical shaped which was related to the unreacted MgH_2. However, with an increase in temperature to 350°C, the new phase of $TiCl_3$ started to appear. Moreover, SEM/EDX analysis showed that at 350°C and reaction time for 4 hrs (run #1), the high Ti content phase was measured which indicated TiH_2 and confirmed via XRD analysis. The SEM/EDX analyziz for the reduction process above 10hrs and temperature of 400°C showed the large particles in the final products with Ti content about 100%wt which was related to the titanium hydride phases.

Acknowledgements

The authors wish to thank Universiti Sains Malaysia (USM) and Ministry of Education (MOE) of Malaysia for supporting this work. This research was supported primarily by the following grants; MOHE Fundamental Research Grant Scheme (FRGS) grant #203/PBAHAN/6071364 and USM Research University Individual (RUI) grant #1001/PBAHAN/814273. Further support by USM

research grant was entitled Geran Bridging #304/PBAHAN/6316116 and Nippon Sheet Glass Research Grant (NSGRG) (#304/PBA HAN/650360/N120).

References

[1] E.O. Ezugwu, J. Bonney, Y. Yamane, J Mater Process Tech. 134 (2003) 233-253

[2] R.R. Boyer, JOM US. 62 (2010) 21-24

[3] Ervin Tal-Gutelmacher, Dan Eliezer, Mater Trans. 45 (2004) 1594-1600

[4] P.A.T. Olsson, J. Blomqvist, C. Bjerkén, A.R. Massih, Comput. Mater. Sci. 97 (2015) 263-275

[5] G. Crowley, Adv Mater Process. 161 (2003) 25-27

[6] D. J. Fray, Int Mater Rev. 53 (2008) 317-325

[7] C. G. McCracken, C. Motchenbacher, D. P. Barbis, Int J Powder Metall. 46 (2010) 19-26

[8] D.S. Van Vuuren: J. S. Afr. Inst. Min. Metall. 109 (2009) 455–461.

[9] Y. Xia, Z.Z. Fang, T.Y. Zhang, Y. Zhang, P. Sun, Z. Huang: The 13th World Conference on Titanium, California, USA, 2015.

[10] D. S. Van Vuuren: 7th International Heavy Minerals Conference 'What next', The Southern African Institute of Mining and Metallurgy, (2009) 1–7.

[11] M. Qian, F. H. Froes, Titanium Powder Metallurgy: Science, Technology and Applications, first ed., Elsevier, Amsterdam, 2015

[12] Y. Zhang, Z. Z. Fang, Y. Xia, P. Sun, B. V. Devener, M. Free, H. Lefler, S. Zheng, Chem Eng J. 308 (2017) 299–310

[13] S.J. Oosthuizen: J. S. Afr. Inst. Min. Metall. 111 (2011) 199–202

[14] W. Chen, Y. Yamamoto, W.H. Peter, M.B. Clark, S.D. Nunn, J.O. Kiggans, T.R. Muth, C.A. Blue, J.C. Williams and K. Akhtar: J. Alloy. Compd. 541 (2012) 440–447.

[15] C. Doblin, A. Chryss and A. Monch: Key Eng. Mater. 520 (2012) 95–100.

[16] D.S. van Vuuren: Direct titanium powder production by metallothermic processes, in Titanium Powder Metallurgy: Science, Technology and Applications. 2015. p. 69–93.

[17] Z.Z. Fang, S. Middlemas, J. Guo and P. Fan, J. Am. Chem. Soc. 135 (2013) 18248–18251.

[18] E. Ahmadi, S. A. Rezan, N. Baharun, S. Ramakrishnan, A. Fauzi, G. Zhang, Metall Mater Trans B. 45 (2017) 2354-2366

[19] E. Ahmadi, A. Fauzi, H. Hussin, N. Baharun, K. S. Ariffin, S. A. Rezan, Int J Min Met Mater. 24 (2017) 444-454

[20] E. Ahmadi, Y. Yashima, R. O. Suzuki, S. A. Rezan, Metall Mater Trans B. 49 (2018) 1808–1821

[21] M. R. Ardani, A. S. M. Al Janabi, S. Udayakumar, S. A. Rezan, M. N. A. Fauzi, A. R. Mohamed, H. L. Lee, I. Ibrahim, in: G. Azimi, H. Kim, S. Alam, T. Ouchi, N. R. Neelameggham, A. A. Baba (Eds.), Rare Metal Technology 2019, Springer, Cham, 2019, pp. 131-144

[22] S. Udayakumar, A. Sadaqi, N. Ibrahim, M. N. A. Fauzi, S. Ramakrishnan, S. A. Rezan, JPCS. 1082 (2018) 012003-012009

[23] S. Udayakumar, A. Sadaqi, N. Ibrahim, M. N. A. Fauzi, S. Ramakrishnan, S. A. Rezan, JPCS. 1082 (2018) 012037-012043

[24] Z. Z. Fang, P. Fan, S. Middlemas, J. Guo, Y. Zhang, M. Free, A. Sathyapalan, Y. Xia, U.S. Patent Application No. 14/912846, 2016

[25] V. Duz, M. Matviychuk, A. Klevtsov, V. Moxson, Met Powder Rep. 72 (2016) 30-38

[26] V. Duz, V. S. Moxson, A. G. Klevtsov, V. Sukhoplyuyev, Titanium 2013 Conference, Nevada, USA, 2013

[27] C.R.F. Azevedo, D. Rodrigues, F. Beneduce Neto, J Alloy Compd. 353 (2003) 217–227

[28] O. Ivasishin, V. Moxson, in: M. Qian, F. H. Froes (Eds.), Titanium Powder Metallurgy: Science, Technology and Applications, Elsevier, Amsterdam, 2015, pp 117-148

[29] A. Grzech, U. Lafont, P. C. M. M. Magusin, F. M. Mulder, J. Phys. Chem. C. 116 (2012) 26027−26035

[30] O. Palumbo, F. Trequattrini, F.M. Vitucci, A. Bianchin, A. Paolone, J Alloy Compd. 645 (2014) S239-S241

[31] A. Roine, "Outokumpu HSC Chemistry, Chemical reaction and equilibrium software with extensive thermochemical database", Finland Outokumpu Research Oy, 2006

[32] L. P. Ma, X. D. Kang, H. B. Dai, Y. Liang, Z. Z. Fang, P. J. Wang, P. Wang, H. M. Cheng, Acta Mater. 57 (2009) 2250–2258

[33] S. J. Gao, L. J. Huang, J Alloy Compd. 293–295 (1999) 412–416

[34] G. J. Kipouros, D. R. Sadoway, J. Light Me. 1 (2001) 111-117

[35] Q. Huang, G. Lu, J. Wang, J. Yu, J Anal Appl Pyrolysis. 91 (2011) 159–164